malocclusion incisors, and epicanthic folds, as seen in WHS. These results indicate that the haploinsufficiency of the *Whsc1* gene in mice causes defects as a part of WHS.

To investigate developmental defects, we stained the embryonic cartilage with alcian blue and the ossified bone with alizarin red, and found several deficiencies in midline fusion in mutant E18.5 embryos. In normal mice, the sternums fuse by E17.5 and subsequent ossification centres typically arise. *Whsc1*$^{-/-}$ mice did not show any ossification centres at E18.5 (Fig.3b). Even in *Whsc1*$^{+/-}$ mice, the appearance of ossification centres was markedly delayed. We further found incidences of cleft palate in *Whsc1*$^{-/-}$ mice, as is also seen in WHS.

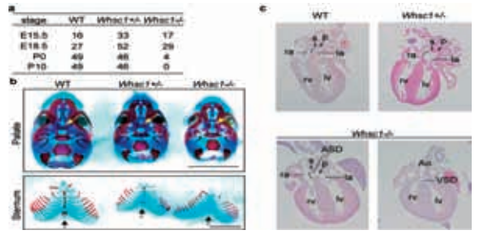

Figure 3. The *Whsc1* gene is required for normal mouse development. **a,** Genotype analysis of embryos and neonates from *Whsc1*$^{+/-}$ intercrosses. **b,** Skeletal preparation of E18.5 embryos. Cartilage was stained with alcian blue and ossified bone was stained with alizarin red. Yellow arrows, palates; black arrows, sternum. Scale bar, 5 mm. **c,** Histological analysis of *Whsc1* mutant embryonic hearts. Frontal sections from E18.5 embryos were stained with hematoxylin and eosin. Atrial septal defects (ASD) and ventricular septal defects (VSD) were observed in E18.5 *Whsc1*$^{-/-}$ embryos. The foramen ovales of E18.5 *Whsc1*$^{+/-}$ embryos were larger than those of wild-type embryos. Hypoplasia of the septum secundum was observed in E18.5 *Whsc1*$^{+/-}$ embryos (bracket). Ao, aortic root; lv, left ventricle; rv, right ventricle; la, left atrium; ra, right atrium; p, septum primum; s, septum secundum.

Whsc1 is required for the appropriate transcription of *Nkx*2-5–dependent genes.

We next analyzed cardiovascular development in *Whsc1* mutant embryos, because WHS patients often have congenital heart defects, including atrial and ventricular septal defects (ASD/VSD). In wild-type mice at E18.5, the septum primum had grown to reach the atrial endocardium (Fig.3c). We found that all *Whsc1*$^{-/-}$ hearts showed an ASD, and half also exhibited a membranous VSD (Fig.3c, bottom). Hypoplasia of the septum secundum was observed more frequently than in wild-type mice, even in heterozygous mutant mice (Fig.3c). These results suggest that the loss of *Whsc1* causes a wide variety of midline defects, including the heart lesions seen in WHS, and leads to death after birth.

To examine whether a specific molecular interaction exists between Whsc1 and the cardiac transcription factors, we performed coimmunoprecipitation assays using an anti-Whsc1 antibody and found a physical interaction between Whsc1 and a central transcriptional regulator of cardiac development, Nkx2-5 (Fig.4a) (*3*). Whsc1 and Nkx2-5 were enriched at the first exon of *Pdgfra*, one of the up-regulated genes in *Whsc1*$^{-/-}$ hearts (Fig. 4b, c, d, and e).

Finally, we crossed *Whsc1*$^{+/-}$ and *Nkx2-5*$^{+/-}$ mice to investigate their functional link *in vivo*. Neither *Nkx2-5*$^{+/-}$ nor *Whsc1*$^{+/-}$ single-heterozygous mutant mice exhibited any significant defects in the septum primum or the interventricular septum of their hearts at E18.5. In contrast, we found both an ASD and a VSD in one third of embryonic hearts from *Whsc1*$^{+/-}$*Nkx2-5*$^{+/-}$ double-heterozygous mutants (Fig.4f). Thus, we have demonstrated here the genetic interaction between Whsc1 and Nkx2-5 during atrial/ventricular septal formation. Our findings partly explain that the congenital heart malformations seen in both *Whsc1* mutant mice and WHS patients are caused by dysfunction of Nkx2-5.

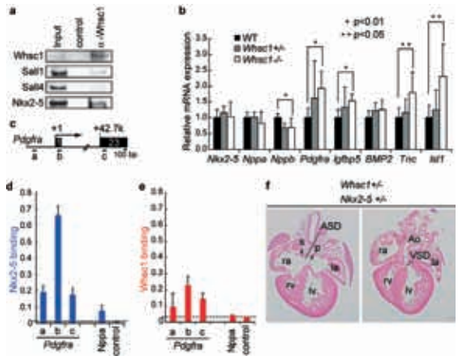

Figure 4. Whsc1 is required for the appropriate transcription of *Nkx2-5*–dependent genes. **a,** Whsc1 complex was immunoprecipitated from the nuclear extracts of E12.5 hearts using an anti-Whsc1 or control antibody and analyzed by immunoblotting with the indicated antibodies. **b,** Quantitative RT-PCR analysis of the expressions of *Nkx2-5* and *Nkx2-5*-dependent genes. **c,** Schematic representation of the *Pdgfra* gene. Locations of genomic regions analyzed by ChIP assays are indicated. a, promoter; b, first exon; c, last exon 23. **d, e,** Native ChIP assays examining the occupancy of Nkx2-5 (d) and Whsc1 (e) at the *Pdgfra* regions indicated in (c). **f,** Histological analysis of *Whsc1*$^{+/-}$ and *Nkx2-5*$^{+/-}$ embryonic hearts. Frontal sections from E18.5 embryos were stained with hematoxylin and eosin.

Conclusion

We have revealed a developmental and pathological link between H3K36 trimethyltransferase and transcription factors. Interactions of multiple transcription factors with Whsc1 could account for the variability of defects caused by the *Whsc1* deficiency. Our studies provide new insights into the molecular mechanism of Nkx2-5-dependent gene regulation in hearts, in which Whsc1 negatively modulates the transcriptional activity of Nkx2-5. Since Nkx2-5 regulates transcription by cooperating with various cardiac transcription factors, Whsc1 might function in the tuning of these transcriptional networks. Our findings point to a new direction for the understanding and treatment of dysregulated transcription, in which WHSC1 functions together with developmental transcription factors to prevent transcriptional pathophysiologies.

References

[1] Bergemann, A. D., Cole, F. & Hirschhorn, K. The etiology of Wolf-Hirschhorn syndrome. Trends Genet. 21, 188-195 (2005).

[2] Stec, I. et al. WHSC1, a 90 kb SET domain-containing gene, expressed in early development and homologous to a Drosophila dysmorphy gene maps in the Wolf-Hirschhorn syndrome critical region and is fused to IgH in t(4;14) multiple myeloma. Hum. Mol. Genet. 7, 1071-1082 (1998).

[3] Prall, O. W. et al. An Nkx2-5/Bmp2/Smad1 negative feedback loop controls heart progenitor specification and proliferation. Cell 128, 947-959 (2007).

A High-Resolution Structure of the Pre-microRNA Nuclear Export Machinery

Paper in journals : this is the first page of a paper published in ***Science.***
[*Science*] 326, 1275-1279 (2009)

REPORTS

A High-Resolution Structure of the Pre-microRNA Nuclear Export Machinery

Chimari Okada,[1,6]* Eiki Yamashita,[1]* Soo Jae Lee,[2]† Satoshi Shibata,[3] Jun Katahira,[3,4] Atsushi Nakagawa,[1] Yoshihiro Yoneda,[3,4,5]† Tomitake Tsukihara[1,6]†

Nuclear export of microRNAs (miRNAs) by exportin-5 (Exp-5) is an essential step in miRNA biogenesis. Here, we present the 2.9 angstrom structure of the pre-miRNA nuclear export machinery formed by pre-miRNA complexed with Exp-5 and a guanine triphosphate (GTP)–bound form of the small nuclear guanine triphosphatase (GTPase) Ran (RanGTP). The x-ray structure shows that Exp-5:RanGTP recognizes the 2-nucleotide 3′ overhang structure and the double-stranded stem of the pre-miRNA. Exp-5:RanGTP shields the pre-miRNA stem from degradation in a baseball mitt–like structure where it is held by broadly distributed weak interactions, whereas a tunnel-like structure of Exp-5 interacts strongly with the 2-nucleotide 3′ overhang through hydrogen bonds and ionic interactions. RNA recognition by Exp-5:RanGTP does not depend on RNA sequence, implying that Exp-5:RanGTP can recognize a variety of pre-miRNAs.

Mature microRNAs (miRNAs), short noncoding RNAs present in a wide range of eukaryotes (*1*, *2*), play important roles in the regulation of biological processes including development, cell proliferation, cell differentiation, apoptosis, transposon silencing, and antiviral defense (*3*–*6*). miRNA biogenesis (*7*) begins in the nucleus, where capped and polyadenylated primary miRNAs, several kilobases in length, are transcribed. These are processed by the nuclear ribonuclease (RNase) III enzyme Drosha to generate ~65-nucleotide (nt) pre-miRNAs that have stem-loop structures containing 2-nt 3′ overhangs. Exp-5 translocates pre-miRNAs from the nucleus to the cytoplasm through the nuclear pore complex (*8*–*12*). In the cytoplasm, the pre-miRNAs are further processed by the cytoplasmic RNase III enzyme Dicer, which excises a ~22–base pair (bp) RNA duplex. One strand of the duplex binds to its target mRNA with imperfect complementarity, usually within the target's 3′ untranslated region, assisted by the RNA-induced silencing complex (*7*).

Exp-5 facilitates miRNA biogenesis not only by acting as the nuclear export factor for pre-miRNAs but also by protecting pre-miRNAs from digestion by nucleases. Loss of Exp-5 results in the loss of cytoplasmic miRNA expression without nuclear accumulation of pre-miRNAs (*10*). Pre-miRNA binding to Exp-5 requires the guanine triphosphatase (GTPase) Ran (RanGTP). The Exp-5:RanGTP:pre-miRNA heteroternary complex formed in the nucleus is exported to the cytoplasm. Ran GTPase–activating protein, which promotes guanine triphosphate (GTP) hydrolysis in conjunction with RanBP1 and/or RanBP2, is exclusively localized in the cytoplasm and triggers the conformation change of Ran to induce release of the pre-miRNA cargo from Exp-5 (*13*, *14*).

Here, we report the structure of the Exp-5:RanGTP:pre-miRNA complex at 2.9-Å resolution (Fig. 1A and fig. S1). This complex contains full-length human Exp-5, canine RanGTP residues 1 to 176 (removal of residues 177 to 216 stabilizes the GTP-bound conformation), and the 48-nt human pre-miRNA-30a stem domain, which includes the 2-nt 3′ overhang (nucleotide numbers 1 to 24 and 40 to 63 of human pre-miRNA-30a). Phase information used for the crystal structure analysis was derived from crystals containing Se-methionine–substituted Exp-5, and the RNA sequence was assigned from the Br anomalous signal information in crystals containing pre-miRNA 5-bromo-oxyuracil derivatives. The structure was refined to an *R* factor of 0.247 and free *R* factor of 0.312, and phasing statistics are provided in table S1. We modeled 1082 of 1204 residues of Exp-5. Several loop regions in the 20 HEAT repeats and 55 residues at the C terminus could not be modeled (details in fig. S1), and 13 residues at the C terminus were modeled as a polyalanine α helix. The residues 1 to 6 of Ran were not modeled because of their disordered structure. Electron density for the pre-miRNA was detected for nucleotides 1 to 11, 14 to 24, and 40 to 63 (fig. S2). The pre-miRNA-30a adopted a typical A-form RNA helical structure, 60 Å in length and 20 Å in diameter.

The Exp-5:RanGTP:pre-miRNA complex is an ellipsoid with dimensions of 65 Å by 80 Å by 110 Å. The crystal structure contains two ternary complexes, labeled A and B, in the asymmetric unit, which are essentially similar [root mean square (RMS) of 1.84 Å, where B is slightly more open than A] and present the same recognition modes for the pre-miRNA. Detailed structural comparison of ternary complexes A and B is described in (*15*). The structure of Exp-5 resembles a tightly wound spring, as seen in other members of the importin-β family. Such conformations are expected to be intrinsically flexible, so small changes in the relative orientation of successive HEAT repeats could cumulatively generate substantial changes in the helicoidal pitch (*16*). Ternary complex A yielded more contrast in its electron density map than did complex B; thus, all structural descriptions of the ternary complex in the following discussion will be restricted to ternary complex A. The Exp-5:RanGTP complex forms a baseball mitt–like structure in which the pre-miRNA is packed (Fig. 1B). A tunnel-like structure at the bottom of the mitt connects the inner space of the mitt with the outer space (Fig. 1B).

The pre-miRNA stem is caught in the mitt formed by the Exp-5:RanGTP complex (Fig. 1), whereas the 15-Å 2-nt 3′ overhang is inserted into a tunnel formed from elements of HEAT repeats 12 to 15 (Figs. 2 and 3 and fig. S3). The inner surface of the tunnel is positively charged

[1]Institute for Protein Research, Osaka University, 3-2 Yamadaoka, Suita, Osaka 565-0871, Japan. [2]College of Pharmacy, Chungbuk National University, Gaeshin-dong, Heungduk-gu, Cheongju City, Chungbuk, Korea. [3]Department of Frontier Biosciences, Graduate School of Frontier Biosciences, Osaka University, 1-3 Yamada-oka, Suita, Osaka 565-0871, Japan. [4]Department of Biochemistry, Graduate School of Medicine, Osaka University, 2-2 Yamada-oka, Suita, Osaka 565-0871, Japan. [5]Japan Science and Technology Agency (JST), Core Research for Evolutional Science and Technology (CREST), Graduate School of Frontier Biosciences, Osaka University, 1-3 Yamada-oka, Suita, Osaka 565-0871, Japan. [6]Department of Life Science, University of Hyogo, 3-2-1 Koto, Kamighori, Akoh, Hyogo 678-1297, Japan.

*These authors contributed equally to this work.
†To whom correspondence should be addressed. E-mail: sjlee@chungbuk.ac.kr (S.J.L.); yyoneda@anat3.med.osaka-u.ac.jp (Y.Y.); tsuki@protein.osaka-u.ac.jp (T.T.)

▲From ***Science***, 326, Okada, C. et al., A High-Resolution Structure of the Pre-microRNA Nuclear Export Machinery, 1275-1279, 2009. Reprinted with permission from AAAS.

The following is a comment on the published paper shown on the preceding page.

Structure of Pre-microRNA Nuclear Export Machinery

OKADA-JIKO Chimari and YAMASHITA Eiki
(Institute for Protein Research)

Introduction

Mature microRNAs (miRNAs), short noncoding RNAs present in a wide range of eukaryotes, fungi, plants, and animals (1, 2), play important roles in the regulation of biological processes including development, cell proliferation, cell differentiation, apoptosis, transposon silencing, and antiviral defense (3-6). miRNA biogenesis (7) begins in the nucleus, where capped and polyadenylated primary-miRNAs, several kilobases in length, are transcribed. These are processed by the nuclear RNase III enzyme Drosha to generate ~65 nt pre-miRNAs that have stem-loop structures containing 2-nt 3' overhangs. Exportin-5 (Exp-5) translocates pre-miRNAs from the nucleus to the cytoplasm through the nuclear pore complex (8-12). In the cytoplasm, the pre-miRNAs are further processed by the cytoplasmic RNase III enzyme Dicer, which excises a ~22 bp RNA duplex. One strand of the duplex binds to its target mRNA with imperfect complementarity, usually within the target's 3'-untranslated region, assisted by the RNA-induced silencing complex (7). Exp-5 facilitates miRNA biogenesis not only by acting as the nuclear export factor for pre-miRNAs but also by protecting pre-miRNAs from digestion by nucleases. Pre-miRNA binding to Exp-5 requires the guanine triphosphatase Ran (RanGTP). The Exp-5:RanGTP:pre-miRNA hetero-ternary complex formed in the nucleus is exported to the cytoplasm. We report the structure of the Exp-5:RanGTP:pre-miRNA ternary complex at 2.9 Å resolution.

Overall structure of the Exp-5:RanGTP;pre-miRNA complex

The crystal structure of the Exp-5:RanGTP:pre-miRNA complex, which contains full-length human Exp-5, canine RanGTP residues 1–176 (removal of residues 177–216 allows adoption of a GTP-bound conformation), and the human pre-miRNA-30a stem domain consisting of 48 nt, including the 2-nt 3' overhang (nucleotide numbers 1–24 and 40–63 of human pre-miRNA-30a), is presented in Fig. 1. The structure of Exp-5 contains 20 HEAT repeats. The pre-miRNA-30a adopts a typical A-form RNA helical structure, 60 Å in length and 20 Å in diameter. The Exp-5:RanGTP:pre-miRNA complex is an ellipsoidal shape with dimensions 65 x 80 x 110 Å. The Exp-5:RanGTP complex forms a baseball mitt-like structure in which the pre-miRNA is caught (Fig.2). A tunnel like structure at the bottom of the mitt connects the inner space of the mitt with the outer space (Fig.2). The pre-miRNA stem is hold in the mitt formed by the Exp-5:RanGTP complex (Figs.1 and 2), while the 2-nt 3' overhang is inserted into a tunnel formed from elements of HEAT repeats 12-15 (Figs.3 and 4).

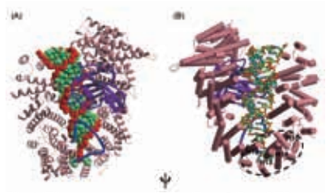

Fig.1 The structure of the Exp-5:RanGTP:pre-miRNA-30a complex. (A) The structure shows human pre-miRNA-30a (red and green) bound to Exp-5 (pink) with RanGTP (purple). The long loop of HEAT15 is shown as a blue wire. At the front of this view, the pre-miRNA is shielded by the long loop of Exp-5 and RanGTP. (B) The pre-miRNA molecule is viewed from the front open side. The 2-nt 3′ overhang structure (circled black) has many interactions with HEAT12–15.

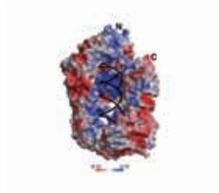

Fig.2 Electrostatic surface potentials of Exp-5:RanGTP. The potentials are represented in a color gradient from red to blue for the vertex with the potential from -0.1 V to 0.1 V. The black backbone represents the stem moiety of the pre-miRNA.

A tunnel captures the 2-nt 3′ overhang of pre-miRNA

The 2-nt 3' overhang structure is a characteristic feature of pre-miRNA. The protruding unpaired 2-nt 3' end is inserted deep into the tunnel constructed from the loop and the inner helix of HEAT12, the loop and the N-terminal end of the inner helix of HEAT13, the N-terminal region of the inner helix of HEAT14, the C-terminal half loop, and the N-terminal region of the inner helix of HEAT15. The tunnel is 15 Å in length, and its shortest diameter is 10 Å wide. The inner surface of the tunnel is positively charged (Figs.2 and 4B) and probably stabilizes the negatively charged 2-nt 3' overhang structure. At the tunnel entrance, located at the bottom of the mitt, Arg602 (HEAT12), which is engaged in tight π-π stacking with the base pair of G1:C61 (Fig.4), sterically blocks the double-stranded stem from entering the tunnel. The 2-nt 3' overhang structure in the tunnel is stabilized by a number of short interatomic interactions with amino acid residues of Exp-5, as shown in Fig. 4. Because all interactions involve atoms of the sugar-phosphate backbone, 2-nt 3' overhang recognition by Exp-5 is independent of RNA sequence.

Fig.3 Intermolecular interactions in the Exp-5:RanGTP:pre-miRNA-30a complex are shown schematically. The pre-miRNA is colored in red and light brown, where red regions interact with more basic residues of Exp-5 than light brown regions. A pink double-octagon represents each HEAT repeat. Exp-5 residues shown in red are involved in the recognition of the 2-nt 3′ end of the pre-miRNA, and black residues indicate interactions with the double-stranded stem of the pre-miRNA. Green residues indicate interactions between Exp-5 and RanGTP.

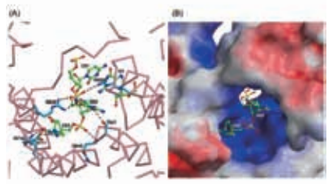

Fig.4 The structure of 2-nt 3′ overhang of the pre-miRNA in the tunnel viewed from outside of the Exp-5 molecule. (A) Hydrogen bonds or salt bridges in the tunnel are represented by broken lines. Exp-5 is clored in pink for Cα, deep blue for N, red for O and sky blue for the other side chain atoms. RNA is colored in deep blue for N, red for O, yellow for P and green for the other atoms. (B) Electrostatic potential is represented as in Fig. 2.

According to an in vitro Exp-5 binding assay, mutants containing a 2–5 nt 5' overhang exhibited reduced binding affinity (13). A model of such a mutant with a 5' overhang built with the crystal structure as template suggests that the 3' end of the stem would sterically clash with HEAT11-12 if the 5' overhang would be inserted into the tunnel (Fig.5). The modeling thus suggests how Exp-5 might discriminate between 3' and 5' end structures.

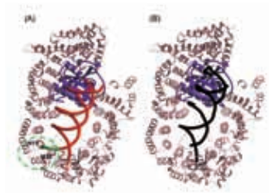

Fig.5 The predicted model of a 2-nt 5′ overhang double-stranded RNA (A) is depicted in the same orientation as Exp-5:RanGTP:pre-miRNA (B). The model of 2-nt 5′ overhang double-stranded RNA is colored in green for its 5′ overhang region and red for the other part. The 2-nt 5′ overhang is inserted into and the 3′ end of the stem sterically clashes with HEAT 11 and 12 in the predicted structure. The clashed regions are highlighted by the green dotted circle.

Exp-5:RanGTP complex as a molecular mitt for double-stranded RNAs

Although Exp-5 is an acidic protein with pI=5.6, the protein has localized positive charges from 27 basic residues on the inner surface of the mitt that interact with the negatively charged dsRNA (Fig.2). Of the 27 basic residues on the inner surface of the mitt, 11 arginine residues, 1 lysine residue, and 1 histidine residue are involved in 21 interactions with the 16 bp stem of the pre-miRNA molecule within an inter-atomic distance of 4 Å. The interacting residues of Exp-5 are distributed broadly on the inner helices of HEAT6-19 and a loop of HEAT15 to recognize the outer phosphodiester group of the pre-miRNA 16 bp stem (Fig. 3). The dipole moment of the inner helix of HEAT19 is attracted to the negative charge of the double-stranded pre-miRNA, as also appears in Xenopus laevis RNA-binding protein A (14). The interatomic distances between the RNA stem and the protein within the mitt region are significantly longer than those within the tunnel region, and the number of contacts per nucleotide in the mitt is significantly fewer than those in the tunnel. Thus, the 16 bp stem of the pre-miRNA, 45 Å in length, is most likely roughly recognized through a broad range of positively charged inner surface residues of the Exp-5:RanGTP mitt.

This structural study indicates that pre-miRNA interacts with Exp-5:RanGTP mainly through ionic interactions in an RNA sequence independent manner. RNA sequence-independent recognition by Exp-5:RanGTP is supported by in vitro binding assays, which demonstrated that the binding of pre-miRNA to Exp-5 occurs through the double-stranded stem and protruded 2-nt 3' overhang, but does so independently of RNA sequence (15).

Protection from RNase

Since both 3' and 5' ends of the pre-miRNA are completely shielded in the tunnel, the pre-miRNA is protected from digestion by exonucleases. It is clear from the structure of Exp-5:RanGTP:pre-miRNA that Exp-5:RanGTP prevents an endonuclease from approaching the pre-miRNA in the ternary complex (Fig.1). Exp-5:RanGTP surrounds the pre-miRNA on four sides, protecting it from ribonuclease digestion during export from the nucleus to the cytoplasm. Consistent with this, cytoplasmic miRNA expression is controlled by Exp-5 expression levels, and low Exp-5 expression leads to nuclear degradation of pre-miRNAs (10). Thus, Exp-5:RanGTP may act as both a nuclear export carrier and a molecular stabilizer for pre-miRNAs.

Recognition of other small structural RNAs by Exp-5:RanGTP

It is known that Exp-5 exports not only pre-miRNAs but also other small structured RNAs, such as tRNAs, human Y1 RNA, and adenovirus VA1 RNA, all of which have 3' overhang structures (16, 17). Formation of the corresponding Exp-5:RanGTP:RNA complexes was examined by building structural models of the ternary complexes for these RNAs using the ternary complex of Exp-5:RanGTP:pre-miRNA as a template. These small RNAs could be efficiently packed into both the basic inner surface of the mitt and the tunnel. In the resulting models, the tunnel exhibiting highest positive charge of the molecule recognizes a 3' overhang structure carrying negative charge; the inner basic surface of the mitt surrounds the sugar-phosphate backbone of double-stranded stem moieties; and finally, the mitt accommodates small protrusions at the center of the stem in the mitt by low-energy conformational changes of Exp-5 created by a spring-like movement.

References

[1] R. C. Lee, R. L. Feinbaum, V. Ambros, *Cell* **75**, 843-54 (1993).
[2] B. Wightman, I. Ha, G. Ruvkun, *Cell* **75**, 855-62 (1993).
[3] V. Ambros, *Nature* **431**, 350-5 (2004).
[4] G. B. Ruvkun, *Harvey Lect* **99**, 1-21 (2003).
[5] B. R. Cullen, ***Nature*** 457, 421-5 (2009).
[6] A. Ventura, T. Jacks, *Cell* **136**, 586-91 (2009).
[7] V. N. Kim, J. Han, M. C. Siomi, *Nat Rev Mol Cell Biol* **10**, 126-39 (2009).
[8] A. M. Brownawell, I. G. Macara, *J Cell Biol* **156**, 53-64 (2002).
[9] E. Lund, S. Guttinger, A. Calado, J. E. Dahlberg, U. Kutay, *Science* **303**, 95-8 (2004).
[10] R. Yi, Y. Qin, I. G. Macara, B. R. Cullen, *Genes Dev* **17**, 3011-6 (2003).
[11] M. T. Bohnsack, K. Czaplinski, D. Gorlich, *Rna* **10**, 185-91 (2004).
[12] S. Shibata et al., *Nucleic Acids Res* **34**, 4711-21 (2006).
[13] Y. Zeng, B. R. Cullen, *Nucleic Acids Res* **32**, 4776-85 (2004).
[14] J. M. Ryter, S. C. Schultz, *Embo J* **17**, 7505-13 (1998).
[15] Y. Zeng, B. R. Cullen, *Nucleic Acids Res* **32**, 4776-85 (2004).
[16] C. Gwizdek et al., *J Biol Chem* **278**, 5505-8 (2003).
[17] A. Calado, N. Treichel, E. C. Muller, A. Otto, U. Kutay, *Embo J* **21**, 6216-24 (2002).